December, 1983

LIDS-P-1299
(Revised)

APPLICATION OF THE SCHUR ALGORITHM TO THE INVERSE PROBLEM FOR A LAYERED ACOUSTIC MEDIUM

by

Andrew E. Yagle* and Bernard C. Levy**

Laboratory for Information and Decision Systems
Department of Electrical Engineering and Computer Science
Massachusetts Institute of Technology
Cambridge, MA 02139

*The work of this author was supported by the Exxon Education Foundation.

**The work of this author was supported by the Air Force Office of Scientific Research under Grant AFOSR-82-0135.

ABSTRACT

The Schur algorithm is a signal processing algorithm which works on a layer-stripping principle. Its time-domain version, the fast Cholesky recursion, is a fast and efficient algorithm well-suited for high-speed data processing. In this paper, these algorithms are applied to the inverse problem for a continuous layered acoustic medium. Three different excitations of the medium are considered: impulsive plane waves at normal incidence; impulsive plane waves at oblique incidence; and spherical waves emanating from an impulsive point source. The fast algorithms obtained for each of these problems seem to be computationally superior to past work done on these problems that employed Gelfand-Levitan theory to reconstruct the potential of a Schrodinger equation.

INTRODUCTION

The one-dimensional inverse acoustic problem consists of probing a continuous layered medium (e.g. the ocean floor) with impulsive waves, and determining the profiles of the density $\rho(x)$ and local speed of sound $c(x)$ from the reflected waves measured at the surface. The medium is assumed to be laterally homogeneous, so that material parameters of the medium vary only with depth. Three different types of excitations are used to probe the medium: impulsive plane waves at normal incidence to the medium; impulsive plane waves incident at an angle to the medium; and spherical waves emanating from an impulsive point source. By measuring the reflection response of the medium to these waves at the surface, profiles of the medium parameters are obtained.

Much of the previous work on this problem for the case of plane waves at normal incidence has consisted of deriving a Schrodinger equation from the basic acoustic and stress-strain equations, and then reconstructing the potential appearing in this equation by using the Gelfand-Levitan procedure (Ware and Aki[1], Newton[2], Berryman and Greene[3]). Coen[4] has shown that the obliquely incident plane wave problem can be transformed into the normal incidence problem. Coen[5] has also shown that the point source problem can be reduced to the obliquely incident plane wave problem. However, all of these approaches involve the Gelfand-Levitan procedure (Faddeev[6]), which requires the solution of a Marchenko integral equation. This is a serious handicap to achieving computational efficiency in processing data, for reasons to be discussed later.

In this paper the Schur algorithm is used to solve the one-dimensional inverse acoustic problem for all three excitations, obviating the need for the Gelfand-Levitan procedure and its attendant Marchenko integral

equation. The Schur algorithm is a fast algorithm well-suited, after transformation to the time domain and after discretization, to high-speed data processing. Further, the quantities in the Schur algorithm may be physically interpreted as upgoing and downgoing waves in the sense of Claerbout.[7] This also happens when the discrete form of this algorithm is used to solve the discrete layered (Goupillaud) medium problem for plane waves at normal incidence, and the resulting "dynamic deconvolution" procedure is well known (see Berryman and Greene[3] and Robinson[8]). Here, a continuous-parameter dynamic deconvolution procedure is applied not only to the problem for plane waves at normal incidence, but also for plane waves at oblique incidence and for an impulsive point source. The latter two applications are, to our knowledge, new to the literature.

The Schur algorithm is an example of a layer stripping algorithm, in which an impulse is used to probe a scattering medium, and where the medium is reconstructed layer by layer. This algorithm works as follows. The upgoing and downgoing waves at the surface are known (measured), and the first reflection of the impulse yields information about the medium immediately beneath the surface (at depth Δ). This information is then used to update the waves at this depth. The problem is now the same as the original problem, except that it starts at depth Δ instead of at the surface. Since the impulse continues to propagate down through the medium, this procedure can be repeated, reconstructing the medium parameters with increasing depth. The concept of using an impulse to probe the medium in this way has been used by Symes[9], Santosa and Schwetlick[10], and Bube and Burridge[11]; however their results were limited to the case of plane waves at normal incidence.

Unless otherwise specified, all quantities in this paper are scalars. Partial derivatives are indicated by subscripting the appropriate dependent variables.

I. THE SCHUR ALGORITHM

The Schur algorithm is a fast algorithm which finds frequent application in solving inverse scattering problems (Yagle and Levy[12], Dewilde et al.[13]). In addition to enabling fast data processing, the Schur algorithm is expressed in terms of quantities having scattering interpretations, such as waves and reflectivity functions. This motivates the application of the Schur algorithm to the inverse acoustic problem.

The Schur algorithm arises from the study of the <u>two-component wave system</u> (Yagle and Levy[12], Bruckstein et al.[14])

$$q_{1x}(x,t) + q_{1t}(x,t) = -r(x)q_2(x,t) \tag{1a}$$

$$q_{2x}(x,t) - q_{2t}(x,t) = -r(x)q_1(x,t) \quad . \tag{1b}$$

Note that if $r(x) = 0$ these equations are simply propagation equations for up- and down-going waves travelling at unit velocity. The <u>reflectivity function</u> $r(x)$ represents the effect the scattering medium has on these waves.

Now, let the downgoing wave $q_1(x,t)$ contain a probing impulse, representing an experiment in which the impulse is used to initiate the waves. Then, by causality, both the upgoing and downgoing waves must be zero for $t<x$, since the impulse will not have had time to reach depth x. Thus, we may write

$$q_1(x,t) = b\delta(t-x) + \tilde{q}_1(x,t)1(t-x) \tag{2a}$$

$$q_2(x,t) = \tilde{q}_2(x,t)1(t-x) \tag{2b}$$

where $1(\cdot)$ is the unit step function. Substituting (2) in (1) yields

$$r(x) = 2q_2(x,x)/b \quad . \tag{3}$$

The set of equations (1), (3) is the continuous-parameter fast Cholesky recursion. In Section III it is shown how these equations may be discretized. The resulting algorithm is quite fast, and consists of updating $q_1(x,t)$ and $q_2(x,t)$ in x and t, yielding r(x) by (3). In the sequel, the impulse scale factor b is dropped for convenience.

We now consider matters in the frequency domain. Taking the Fourier transform of (1) yields

$$\hat{q}_{1x} = -j\omega\hat{q}_1(x,\omega) - r(x)\hat{q}_2(x,\omega) \tag{4a}$$

$$\hat{q}_{2x} = -r(x)\hat{q}_1(x,\omega) + j\omega\hat{q}_2(x,\omega) \quad . \tag{4b}$$

This is the two-component wave system in the form in which it will be derived for the various inverse problems considered in this paper. Once this form has been obtained for a problem, the algorithms discussed in this section are all immediately applicable, for waves having the form given by (2).

The wave interpretations for $\hat{q}_1(x,\omega)$ and $\hat{q}_2(x,\omega)$ suggests defining the reflection coefficient representing the medium deeper than depth x:

$$\hat{R}(x,\omega) = \hat{q}_2(x,\omega)/\hat{q}_1(x,\omega) \quad . \tag{5}$$

$\hat{R}(x,\omega)$ is the transfer function between the downgoing and upgoing waves at depth x. Substituting (5) in (4) yields the Riccati equation

$$\hat{R}_x = 2j\omega\hat{R}(x,\omega) + r(x)(\hat{R}(x,\omega)^2 - 1) \tag{6}$$

and an initial-value theorem argument (see Bruckstein et al.[14]) shows that

$$r(x) = \lim_{\omega \to \infty} 2j\omega \hat{R}(x,\omega) \quad . \tag{7}$$

The set of equations (4), (5), (7) constitutes the Schur algorithm, and the set of equations (6), (7) constitutes a continuous-parameter dynamic deconvolution algorithm. The discretized version of the Schur algorithm is similar to, but not the same as, the recursions given in Berryman and Greene[3]. The discretized dynamic deconvolution algorithm, in which $\hat{R}(x,\omega)$ is computed for increasing values of x, starting from a measured reflection response $\hat{R}(0,\omega)$, is comparable to the dynamic deconvolution algorithm described in Robinson[8].

II. PLANE WAVES AT NORMAL INCIDENCE -- PROBLEM SET-UP

The problem to be considered in this section is illustrated in Fig. 1 (with θ set equal to zero). Impulsive planar acoustic waves, propagating vertically, are incident on a layered medium from a homogeneous half-space $x<0$ in which the density ρ_0 and local speed of sound c_0 are known. This half-space could, for example, be the ocean above the ocean floor. The layered medium is assumed to be laterally homogeneous, so that material parameters vary only with depth. The reflections or reverberations making their way back to the surface are measured at the surface as a function of time. The goal is to obtain profiles of material parameters as functions of depth x. The actual parameter profiles that can be reconstructed will be identified shortly. The problem set-up will follow that of Ware and Aki[1], Newton[2], and Berryman and Greene[3]. In this section, the procedure followed by these authors is quickly reviewed, for comparison to the Schur algorithm procedure developed in the next section.

The behavior of the medium subjected to waves is assumed to be described by the acoustic equation for fluids

$$\rho(x)\underline{u}_{tt} = -\nabla p(x,y,z,t) \tag{8}$$

and the stress-strain equation

$$p(x,y,z,t) = -\rho(x)c(x)^2\nabla\cdot\underline{u}(x,y,z,t). \tag{9}$$

In these equations $\underline{u}(x,y,z,t)$ is the (vector) displacement, $p(x,y,z,t)$ is the pressure or stress, $\rho(x)$ is density, and $c(x)$ is the local speed of sound. When the medium is subject to plane waves at normal incidence

the problem becomes completely one-dimensional, and (8) and (9) may be replaced by

$$\rho(x)u_{tt} = -p_x \tag{10}$$

$$p(x,t) = -\rho(x)c(x)^2 u_x \tag{11}$$

where $u(x,t)$ is now the (scalar) vertical displacement.

We now change variables from depth x to travel time $\tau(x)$ (Ware and Aki[1]), which is the time it takes for a wave, starting at the top of the medium (x=0), to reach depth x. This is specified by

$$\tau(x) = \int_0^x ds/c(s) \ . \tag{12}$$

We also define the impedance

$$Z(\tau) = (\rho(\tau)c(\tau))^{1/2} \tag{13}$$

and normalized displacement

$$\phi(\tau,t) = Z(\tau)u(\tau,t). \tag{14}$$

Substituting (11) in (10), using (12) - (14), and taking the Fourier transform yields the Schrodinger equation (Ware and Aki[1])

$$\hat{\phi}_{\tau\tau} + \omega^2\hat{\phi}(\tau,\omega) = V(\tau)\hat{\phi}(\tau,\omega) \tag{15}$$

where $\hat{\phi}(\tau,\omega)$ is the Fourier transform of $\phi(\tau,t)$ and we have defined the potential

$$V(\tau) = (1/Z)(d^2Z/d\tau^2). \tag{16}$$

The term "potential" comes from quantum mechanics, wherein the Schrodinger equation is often encountered in inverse scattering problems. The boundary conditions for the Schrodinger equation are

$$\hat{\Phi}(\tau,\omega) = \begin{cases} e^{-j\omega\tau} + \hat{R}(\omega)e^{j\omega\tau} & \tau < 0 \quad \text{(above surface of medium)} \\ \hat{T}(\omega)e^{-j\omega\tau} & \tau \to \infty \quad \text{(at great depth)}, \end{cases} \tag{17}$$

where $e^{-j\omega\tau}$ represents the source impulsive plane wave and $\hat{R}(\omega)e^{j\omega\tau}$ is the reflected wave from the medium that is measured at the surface. So $\hat{R}(\omega)$ is the (measured) reflection frequency response. $\hat{T}(\omega)$ is the (unmeasured) transmission frequency response; the point here is that there are no upgoing waves at great depths.

It should be evident from (15) - (17) that the material parameter profile that may be deduced from $\hat{R}(\omega)$ is precisely $Z(\tau)$; it is not possible to recover separate profiles for the density $\rho(x)$ and local speed of sound $c(x)$ as functions of depth for the normal incidence problem (Ware and Aki[1]). However, it <u>will</u> be possible to recover these <u>separate profiles</u> as functions of depth for the oblique incidence and point-source problems.

Past procedure at this point (Ware and Aki[1], Newton[2], Berryman and Greene[3]) has been to apply the following <u>Gelfand-Levitan</u> procedure (Faddeev[6], Chadan and Sabatier[15]) to the problems specified by eqns.(15) - (17). The steps are as follows:

(1) Measure $\hat{R}(\omega)$ and/or its inverse Fourier transform $R(t)$

(2) Solve the integral equation

$$K(t,\tau) = -R(t+\tau) - \int_{-t}^{\tau} K(z,\tau)R(z+\tau)\,dz, \quad t \leq \tau \tag{18}$$

(3) Compute from the solution of (18) the Schrodinger potential

$$V(\tau) = 2\, dK(\tau,\tau)/d\tau \tag{19}$$

(4) Using $V(\tau)$ from (19), solve the differential equation (16) for $Z(\tau)$, with the initial conditions $Z(0) = (\rho_0 c_0)^{1/2}$, $(dZ/d\tau)(0) = 0$.

Berryman and Greene[3] have pointed out that steps (3) and (4) may be replaced by the single step

$$\rho(\tau)c(\tau)/(\rho(0)c(0)) = 1 + \int_{-\tau}^{\tau} K(z,\tau)\,dz \tag{20}$$

since the differential equation (16) has the same form as the Schrodinger equation (15) with $\omega=0$.

Note that there are no bound states (see Ware and Aki', Newton[2]) in this inverse scattering problem. Then, the integral equation (18) may be discretized and solved by a fast algorithm as in Berryman and Greene[3]. This algorithm has a form similar to the Schur recursions which will be used below to solve the above inverse scattering problem. However, as noted in Bruckstein et al.[14], the recursions obtained by Berryman and Greene correspond to a boundary value problem, whereas the Schur algorithm is formulated as an initial value problem.

Another difference is that the procedure described above requires that

$$\int_0^{\infty} (1+\tau)\,|V(\tau)|\,d\tau < \infty \quad .$$

This condition is not satisfied when the medium is probed obliquely with impulsive plane waves and when the ray path of the probing wave becomes

horizontal, as it will in a sufficiently extreme low-velocity zone and at a turning point, where the ray path is bent back up toward the surface. In this case the equivalent impedance $Z(\tau)$ (to be defined by (35)) becomes infinite, and the reconstruction procedure described above cannot be used. Since turning points generally occur in real-world experiments, this limitation is quite restrictive. Note that Coen's[4] procedure for the non-normal incidence problem requires precritical incidence at all depths (an unrealistic assumption), while Coen's[5] procedure for the point-source problem requires separate procedures for the cases of pre-critical and post-critical incidence. The Schur algorithm solutions to the non-normal incidence and point-source problems remain valid even in the presence of turning points, and thus seem to be more general than previous solutions of these problems.

III. PLANE WAVES AT NORMAL INCIDENCE -- SCHUR SOLUTION

Define the following normalized quantities:

$$\hat{\phi}(\tau,\omega) = Z(\tau)\hat{u}(\tau,\omega) = \text{normalized displacement} \tag{21a}$$

$$j\omega\hat{\phi}(\tau,\omega) = j\omega Z(\tau)\hat{u}(\tau,\omega) = \text{normalized velocity} \tag{21b}$$

$$\hat{\psi}(\tau,\omega) = \hat{p}(\tau,\omega)/Z(\tau) = \text{normalized pressure.} \tag{21c}$$

These normalized quantities now have unit energy (Claerbout[7]). As in Claerbout[7], the following quantities can be interpreted as (respectively) downgoing and upgoing waves:

$$\hat{q}_1(\tau,\omega) = \hat{\psi}(\tau,\omega) + j\omega\hat{\phi}(\tau,\omega) \tag{22a}$$

$$\hat{q}_2(\tau,\omega) = \hat{\psi}(\tau,\omega) - j\omega\hat{\phi}(\tau,\omega). \tag{22b}$$

Taking the Fourier transforms of the acoustic (10) and stress-strain (11) equations, and making the substitutions (12), (13), (21), and (22) yields the two-component wave system

$$\hat{q}_{1\tau} = -j\omega\hat{q}_1 - r(\tau)\hat{q}_2(\tau,\omega) \tag{23a}$$

$$\hat{q}_{2\tau} = -r(\tau)\hat{q}_1(\tau,\omega) + j\omega\hat{q}_2 \tag{23b}$$

where

$$r(\tau) = (1/Z)(dZ/d\tau) = (d/d\tau)\log Z(\tau). \tag{24}$$

Taking the inverse Fourier transforms of (23), and letting $q_1(\tau,t)$ and $q_2(\tau,t)$ have the forms in equations (2) yields, as before, the fast Cholesky equations

$$q_{1\tau} + q_{1t} = -r(\tau)q_2(\tau,t) \tag{25a}$$

$$q_{2\tau} - q_{2t} = -r(\tau)q_1(\tau,t) \tag{25b}$$

$$r(\tau) = 2q_2(\tau,\tau) \tag{25c}$$

which can be propagated recursively, starting from the downgoing and upgoing waves $q_1(0,t)$ and $q_2(0,t)$ which are measured on the surface of the medium. To see this, let the time t and travel time τ be discretized by $t = n\Delta$ and $\tau=m\Delta$, where n and m are positive integers and Δ is the discretization time. Then a simple Euler-Cauchy approximation to the partial derivatives in (24) and (25) yields the following recursive algorithm:

$$Z(\tau+\Delta) = Z(\tau)(1+r(\tau)\Delta) \tag{26a}$$

$$q_1(\tau+\Delta,t+\Delta) = q_1(\tau,t) - r(\tau)q_2(\tau,t)\Delta \tag{26b}$$

$$q_2(\tau+\Delta,\ t-\Delta) = q_2(\tau,t) - r(\tau)q_1(\tau,t)\Delta \tag{26c}$$

$$r(\tau+\Delta) = 2q_2(\tau+\Delta,\tau+\Delta)\ . \tag{26d}$$

The recursion patterns for the q_i are illustrated in Figs. 2a and 2b. We start off knowing these waves at τ for all t, and wish to find the waves at $\tau+\Delta$ for all t. Note that by causality there can be no wave at "depth" τ until the initial excitation has had time to reach that far. Hence, $q_i(\tau,t) = 0$ for $t<\tau$.

The recursions (26) are initialized by measuring the pressure and velocity of the medium at the surface and using (21) and (22). Often, a free surface is assumed, in which case the pressure at the surface is zero. The density $\rho(0)$ and wave speed $c(0)$ at the surface are assumed to be known. The resulting algorithm runs very rapidly on a computer.

The same approach will also work for the oblique plane wave and point source problems, which are discussed next.

IV. PLANE WAVES AT OBLIQUE INCIDENCE

We now consider the problem in which an impulsive plane wave is obliquely incident, at an angle θ to the vertical, on a one-dimensional layered medium. The reflection frequency response $R(\omega)$ is now measured as a function of the horizontal coordinate y (in the normal incidence problem there is of course no horizontal variation of anything). The situation is illustrated in Fig. 1. This problem was solved by Coen[4], who showed how this problem could be transformed to the normal incidence problem and solved using the Gelfand-Levitan procedure. Here, the Schur algorithm will be shown to solve the problem directly, in terms of transformed quantities. In addition, it will be shown that running this experiment twice, at two different angles of incidence, allows the recovery of the separate profiles $\rho(x)$ and $c(x)$ as functions of depth -- a significant improvement over the normal incidence experiment. Since the data from the two experiments are processed in parallel, the resulting algorithm is still quite fast.

An impulsive plane pressure wave incident at angle θ from the vertical has the form $\delta(t-x \cos \theta/c_0 - y \sin \theta/c_0)$ in the homogeneous half-space $x<0$. In the frequency domain, this is $e^{-j(k_x x + k_y y)}$, where $k_x = \omega \cos \theta/c_0$ and $k_y = \omega \sin \theta/c_0$ are the vertical and horizontal wave numbers and $c_0 = c(0)$. The pressure field for $x<0$ is thus

$$\hat{p}(x,y,\omega,\theta) = e^{-jk_y y} \left(e^{-jk_x x} + \hat{R}(\omega,\theta) e^{jk_x x}\right) \tag{27}$$

(compare this to the Schrodinger equation boundary condition (17)). This shows that the reflection frequency response $\hat{R}(\omega,\theta)$ in the time domain has the form

$$R(t,y;\theta) = R(t-y \sin \theta/c_0;\theta) \tag{28}$$

so that theoretically it should only be necessary to measure this response at a single surface point (e.g. y=0). However, in any real-world application it would be a matter of practical necessity to take data for a range of y and filter or stack it to the form (28). This is because any real-world impulsive wave could only be locally planar, while the form of (28) assumes a plane wave of infinite extent.

Taking Fourier transforms of the acoustic (8) and stress-strain (9) equations, and writing the vector equation (8) as two scalar equations results in

$$\rho(x)\omega^2\hat{u}^x(x,y,\omega) = \hat{p}_x \tag{29a}$$

$$\rho(x)\omega^2\hat{u}^y(x,y,\omega) = \hat{p}_y \tag{29b}$$

$$\hat{p}(x,y,\omega) = -\rho(x)c(x)^2(\hat{u}^x_x + \hat{u}^y_y) \tag{29c}$$

where u^x and u^y are the x and y components of the (vector) displacement $\underline{u}(x,y,t)$.

Since the medium properties vary only with depth x, the horizontal wavenumber k_y is preserved, and we may write (following Coen[4])

$$\hat{p}(x,y,\omega) = \hat{\psi}(x,\omega)e^{-jk_y y} \ . \tag{30}$$

Substituting (30) in (29b), and then substituting the result in (29c) eliminates $\hat{u}^y$ and yields, after some algebra,

$$\hat{p}(x,y,\omega)\ (1-(c(x)^2/c_0^2)\sin^2\theta) = -\rho(x)c(x)^2\hat{u}^x_x \ . \tag{31}$$

Next, the following substitutions are made:

$$\cos^2\theta(x) = 1 - (c(x)^2/c_0^2)\sin^2\theta \tag{32}$$

($\theta(x)$ = local angle ray path makes with vertical)

$$c'(x) = c(x)/\cos\theta(x) = \text{local vertical wave speed} \tag{33}$$

$$\tau(x) = \int_0^x ds/c'(s) = \text{vertical travel time to depth } x \tag{34}$$

$$Z(\tau) = (\rho(\tau)c'(\tau))^{1/2} = \text{effective impedance} \ . \tag{35}$$

Note that (32) follows from Snell's law ($\sin\theta(x)/c(x)$ is constant along any ray path), and (33) defines a local vertical wavenumber $k_x(x) = \omega/c'(x)$. Using (32) - (35) in (31) and (29a) yields

$$\hat{p}_\tau = Z^2\omega^2\hat{u}^x(\tau,y,\omega) \tag{36a}$$

$$\hat{u}^x_\tau = -(1/Z^2)\hat{p}(\tau,y,\omega) \tag{36b}$$

and once again defining the downgoing and upgoing waves (as in Claerbout[7])

$$\hat{v}_1(\tau,y,\omega) = \hat{p}(\tau,y,\omega)/Z + j\omega Z\hat{u}^x(\tau,y,\omega) \tag{37a}$$

$$\hat{v}_2(\tau,y,\omega) = \hat{p}(\tau,y,\omega)/Z - j\omega Z\hat{u}^x(\tau,y,\omega) \tag{37b}$$

yields the two-component wave system

$$\hat{v}_{1\tau} = -j\omega\hat{v}_1 - r(\tau)\hat{v}_2 \tag{38a}$$

$$\hat{v}_{2\tau} = -r(\tau)\hat{v}_1 + j\omega\hat{v}_2 \tag{38b}$$

with the reflectivity function $r(\tau)$ defined as

$$r(\tau) = (1/Z)\ (dZ/d\tau) = (d/d\tau)\log Z(\tau) \ . \tag{39}$$

Here y is fixed at whatever value of y $\hat{R}(\omega,y)$ is measured at (e.g. y=0), and θ is a parameter on which all quantities depend.

Note that once again the quantities in the wave system (38) are the Fourier transforms of the downgoing and upgoing waves, so that once again the vertical motion of the medium is decomposed into upgoing and downgoing waves. Of course, horizontally-travelling waves could not furnish any information on the vertical variation of material parameters. Since these waves have the form defined by equations (2), all of the algorithms specified in Section I can now readily be identified for the oblique incidence problem.

Now, suppose this oblique incidence experiment were run twice, for two different angles of incidence θ_1 and θ_2. Two different impedances $Z_1(\tau_1)$ and $Z_2(\tau_2)$, as functions of different vertical travel times τ_1 and τ_2, would be obtained. The reconstruction procedure given in Howard[16] could then be used to recover the separate profiles $\rho(x)$ and $c(x)$ from $Z_1(\tau_1)$ and $Z_2(\tau_2)$. However, further consideration of the layer-stripping idea yields the following procedure for recovering $\rho(x)$ and $c(x)$ while the two Schur algorithms are running, obviating the necessity of waiting for the complete impedances $Z_i(\tau_i)$. This procedure is also much simpler than the computationally cumbersome method of Howard[16].

Let $r_i(x)$ be the reflectivity function associated with the experiment with angle of incidence θ_i (i=1,2), and let $c_i'(x) = c(x)/\cos\theta_i(x)$ be the associated vertical wavespeed. Then

$$r_i(x) = (1/2)(d/dx)\log(\rho(x)c_i'(x)) \quad . \tag{40}$$

Substituting (33) in (34) and differentiating with respect to x yields

$$(d/dx)c_i'(x) = (1/\cos^3\theta_i(x))(dc(x)/dx) \tag{41}$$

Using (41), equation (40) may be rewritten in matrix form as

$$\begin{bmatrix} r_1(x) \\ r_2(x) \end{bmatrix} = \begin{bmatrix} 1/(2\rho(x)) & 1/(2c(x)\cos^2\theta_1(x)) \\ 1/(2\rho(x)) & 1/(2\,c(x)\cos^2\theta_2(x)) \end{bmatrix} \begin{bmatrix} (d/dx)\rho(x) \\ (d/dx)c(x) \end{bmatrix} \tag{42}$$

Inverting (42) yields

$$\begin{bmatrix} (d/dx)\rho(x) \\ (d/dx)c(x) \end{bmatrix} = \frac{\begin{bmatrix} 1/(2c(x)\cos^2\theta_2(x)) & -1/(2c(x)\cos^2\theta_1(x)) \\ -1/(2\rho(x)) & 1/(2\rho(x)) \end{bmatrix}}{d(x)} \begin{bmatrix} r_1(x) \\ r_2(x) \end{bmatrix} \tag{43}$$

where

$$d(x) = (\cos^{-2}\theta_2(x) - \cos^{-2}\theta_1(x))/(4\rho(x)c(x)). \tag{44}$$

This yields the following recursive algorithm for computing $\rho(x)$ and $c(x)$. Discretizing depth as $x=n\Delta$ and time as $t_i = m\Delta/c_i'(x)$ (note that time is discretized differently at each depth and for the two experiments) and assuming (for inductive purposes) knowledge of all quantities at depth x, the update procedure is as follows:

$$\cos\theta_i(x) = (1-(c(x)^2/c_0^2)\sin^2\theta_i)^{1/2} \tag{45}$$

$$d(x) = (\cos^{-2}\theta_2(x) - \cos^{-2}\theta_1(x))/(4\rho(x)c(x)) \tag{46}$$

$$r_i(x) = 2v_2^i(\tau_i,x)\cos\theta_i(x)/c(x) \tag{47}$$

$$\rho(x+\Delta) = \rho(x) + (r_1(x)/\cos^2\theta_2(x) - r_2(x)/\cos^2\theta_1(x))\Delta/(2c(x)d(x)) \tag{48}$$

$$c(x+\Delta) = c(x) + (r_2(x)-r_1(x))\Delta/(2\rho(x)d(x)) \tag{49}$$

$$v_1^i(x+\Delta,\ t+\Delta\cos\theta_i(x)/c(x)) = v_1^i(x,t) - r_i\Delta v_2^i(x,t) \tag{50}$$

$$v_2^i(x+\Delta,\ t-\Delta\cos\theta_i(x)/c(x)) = v_2^i(x,t) - r_i\Delta v_1^i(x,t) \tag{51}$$

$$\tau_i(x+\Delta) = \tau_i(x) + \Delta\cos\theta_i(x)/c(x) \quad . \tag{52}$$

At this point all quantities have been updated to depth $x+\Delta$, so the recursion is complete. Note that there are two sets of recursions running in parallel, each one initialized by the data from one of the two experiments ($i=1,2$).

The reason that the profiles $\rho(x)$ and $c(x)$ can be recovered separately for the oblique incidence problem, but not for the normal incidence problem, is that by running the oblique experiment twice information has been gained along two <u>different</u> ray paths. This option is not available for the normal incidence problem -- there is only one choice for the ray path, since this problem is completely one-dimensional.

Along any given ray path Snell's law shows that

$$\sin\theta(x)/c(x) = \sin\theta_0/c_0 = \text{ray parameter (constant)} \tag{53}$$

so that unless θ is less than the <u>critical angle</u> $\sin^{-1}(c_0/\max c(x))\theta(x)$ will become imaginary at some depth. Physically, this situation results in <u>evanescent waves</u>, in which the pressure field decays exponentially instead of propagating as a wave. The same effect is observed in a waveguide below cutoff. This causes no problems in the Schur algorithm until the ray path actually becomes horizontal, prior to turning back up. When this <u>turning point</u> is reached, $|r(x)| \to \infty$. However, since no new

information can be gained beyond the turning point anyway (the upgoing ray path must be the mirror image of the downgoing path), the Schur algorithm can simply be terminated when $|r(x)|$ exceeds some pre-set value.

This lack of difficulty with the Schur algorithm when $\theta(x)$ become imaginary is in sharp contrast to Coen[4,5], in which the cases of pre-critical ($\theta(x)$ real) and postcritical ($\theta(x)$ imaginary) incidence must be treated separately.

V. IMPULSIVE POINT SOURCE

The third and final problem considered is one in which the one-dimensional layered medium is excited by an impulsive point source. Such a source, on the surface of a homogeneous medium, would generate spherical waves within the medium. For the layered inhomogeneous medium, of course, the waves will only be spherical in the immediate vicinity of the source.

The situation is illustrated in Fig. 3. Note that since the source has circular symmetry, the entire problem does also. Hence the reflection frequency response $\hat{R}(\omega)$ is now measured as a function of the distance r from the impulsive point source.

This problem was solved by Coen[5], who showed how this problem could be transformed to the problem with plane waves at oblique incidence by stacking the data, and then solved as in Coen[4]. Here, it will be shown that a two-component scattering system for the point source problem can be derived in terms of parametrized Hankel-Fourier transforms of the up- and downgoing waves. Two different parametrizations and the recursive algorithm of Section IV, starting with suitably transformed data, may then be used to obtain the separate profiles $\rho(x)$ and $c(x)$.

The cylindrical symmetry of the problem suggests the use of Hankel transforms. The n^{th} order Hankel transform is defined as (Papoulis[17])

$$H_n\{f(r)\} \triangleq \int_0^\infty f(r) J_n(r\xi) r dr = F_n(\xi) \tag{54}$$

where $J_n(\cdot)$ is the n^{th} order Bessel function. Although Hankel transforms of orders zero and one will be used in the derivation, the Schur algorithm will contain quantities that involve Hankel transforms of order zero only.

The signficance of the Hankel transform in problems with circular symmetry is that the two-dimensional Fourier transform of a function with circular symmetry is the same as the Hankel transform of order zero of the function, to a factor of 2π (Papoulis[17]). Specifically,

$$\hat{f}(x,y) = F(u,v) = 2\pi H_0\{f\}((u^2 + v^2)^{1/2}) . \tag{55}$$

It is also true that

$$H_0\{f(r)/r + (\partial/\partial r)f(r)\} = \xi H_1\{f(r)\} \tag{56a}$$

$$H_1\{(\partial/\partial r)f(r)\} = -\xi H_0\{f(r)\} . \tag{56b}$$

This motivates the use of the Hankel transform in the present problem.

Writing the acoustic (8) and stress-strain (9) equations in cylindrical coordinates, taking Fourier transforms, and noting the circular symmetry of the problem (no θ-dependence) yields

$$\rho(x)\omega^2\hat{u}^r(r,x,\omega) = \hat{p}_r \tag{57a}$$

$$\rho(x)\omega^2\hat{u}^x(r,x,\omega) = \hat{p}_x \tag{57b}$$

$$\hat{p}(r,x,\omega) = -\rho(x)c(x)^2(\hat{u}^x_x + \hat{u}^r/r + \hat{u}^r_r) \tag{57c}$$

where u^r and u^x are the r and x (depth) components of the (vector) displacement $\underline{u}$. Note that the u^θ component of $\underline{u}$ does not appear.

Taking Hankel transforms of order zero of (57b) and (57c), and the Hankel transform of order one of (57a) yields

$$\rho(x)\omega^2\hat{U}^r(\xi,x,\omega) = -\xi\hat{P}(\xi,x,\omega) \tag{58a}$$

$$\rho(x)\omega^2\hat{U}^x(\xi,x,\omega) = \hat{P}_x \tag{58b}$$

$$\hat{P}(\xi,x,\omega) = -\rho(x)c(x)^2(\hat{U}^x_x + \xi\hat{U}^r(\xi,x,\omega)) \tag{58c}$$

where

$$\hat{U}^r(\xi,x,\omega) = H_1\{\hat{u}^r(r,x,\omega)\} \tag{59a}$$

$$\hat{U}^x(\xi,x,\omega) = H_0\{\hat{u}^x(r,x,\omega)\} \tag{59b}$$

$$\hat{P}(\xi,x,\omega) = H_0\{\hat{p}(r,x,\omega)\}. \tag{59c}$$

Eliminating $\hat{U}^r$ from (58) yields

$$\rho(x)\omega^2\hat{U}^x(\xi,x,\omega) = \hat{P}_x \tag{60a}$$

$$\hat{P}(\xi,x,\omega)(1-(\xi^2/\omega^2)c(x)^2) = -\rho(x)c(x)^2\hat{U}^x_x \tag{60b}$$

and defining (compare to (32) - (35))

$$c'(x)^2 = c(x)^2/(1-(\xi^2/\omega^2)c(x)^2) \tag{61}$$

$$\tau(x) = \int_0^x ds/c'(s) \tag{62}$$

$$Z(\tau) = (\rho(\tau)c'(\tau))^{1/2} \tag{63}$$

results in the familiar equations (compare to (36))

$$\hat{P}_\tau = Z^2\omega^2\hat{U}^x(\xi,\tau,\omega) \tag{64a}$$

$$\hat{U}^x_\tau = -(1/Z^2)\hat{P}(\xi,\tau,\omega) \ . \tag{64b}$$

Recalling that the Hankel transform of order zero is the two-dimensional Fourier transform of a circularly symmetric function, we may once again define the Hankel-Fourier transforms of the downgoing and upgoing waves (as in Claerbout[7])

$$\hat{V}_1(\xi,\tau,\omega) = \hat{P}(\xi,\tau,\omega)/Z + j\omega Z\hat{U}^x(\xi,\tau,\omega) \tag{65a}$$

$$\hat{V}_2(\xi,\tau,\omega) = \hat{P}(\xi,\tau,\omega)/Z - j\omega Z\hat{U}^x(\xi,\tau,\omega) \tag{65b}$$

yields the two-component wave system

$$\hat{V}_1 = -j\omega\hat{V}_1(\xi,\tau,\omega) - r(\tau)\,\hat{V}_2(\xi,\tau,\omega) \tag{66a}$$

$$\hat{V}_{2\tau} = -r(\tau)\hat{V}_1(\xi,\tau,\omega) + j\omega\hat{V}_2(\xi,\tau,\omega) \tag{66b}$$

with the reflectivity function $r(\tau)$ given by

$$r(\tau) = (1/Z)(dZ/d\tau) = (d/d\ )\ \log Z(\tau). \tag{67}$$

Once again, the waves will have the form defined by equations (2), so all of the algorithms specified in Section I can now be applied to the point source problem.

However, it is still necessary to initiate the algorithm using the given data. One way to do this is to impose the following condition on the independent variables ξ and ω (Coen[5]):

$$\xi = (\omega/c_0)\ \sin\theta \tag{68}$$

where θ is a parameter. Substituting (68) in (61) leads to

$$c'(x)^2 = c(x)^2/(1-(c(x)^2/c_0^2)\sin^2\theta) = c(x)^2/\cos^2\theta(x) \tag{69}$$

which is the same as (32) and (33) in the obliquely incident plane wave problem. Thus the point source problem has been transformed into an obliquely incident plane wave problem, which was solved in the previous section.

To obtain $\hat{R}(\omega,\theta)$, the initial condition for the Schur algorithm for the oblique plane wave problem, from data measured for an impulsive point source, it is necessary to use boundary conditions for the impulsive point source on the oblique plane wave problem solution (27). This is carried out in detail in Coen[5], and we simply repeat the result here:

$$\hat{R}(\omega,\theta) = (1 + k_0\hat{V}(\omega,\theta))/(1-k_0\hat{V}(\omega,\theta)) \tag{70}$$

where

$$k_0 = \rho_0 c_0/b \cos\theta \tag{71a}$$

$$\hat{V}(\omega,\theta) = H\{\hat{v}(r,\omega)\}\big|_{\xi = (\omega/c_0)\sin\theta} \tag{71b}$$

and $\hat{v}(r,\omega)$ is the Fourier transform of the vertical particle velocity measured for an impulsive point source of strength b. It is shown in Coen[5] that the condition (68) amounts to a Radon transform or "slant stack" (Robinson[8]) on the data $v(r,t)$.

In summary: to use the Schur algorithm to solve the impulsive point source problem, proceed as follows:

(1) Run the physical experiment, obtaining the data $v(r,t)$:

(2) Using (70) and (71), transform the data $v(r,t)$ to the artifical data $\hat{R}(\omega,\theta)$, for two different values θ_1, θ_2 of the parameter θ;

(3) Run the recursive algorithm specified by equations (45)-(52) to generate the profiles $\rho(x)$ and $c(x)$.

VI. PERFORMANCE OF THE ALGORITHMS

The basic fast Cholesky algorithm (26) has been proven to be stable by Bultheel[18]. This means that the numerical result of running the algorithm, starting from a given set of data, is the same result as would be obtained by running the algorithm, without roundoff errors, on a slight perturbation of the original data. Since the fast Cholesky algorithm (the time-domain version of the Schur algorithm) forms the core of the algorithms in this paper, it can be expected that they too can be proven stable, although this has not yet been accomplished.

Bube and Burridge[11] have tested the normal-incidence problem algorithm using numerical simulations, and the results are quite good. The algorithm does an especially good job of tracking sharp changes in the impedance profile. The performance of the oblique-incidence and point source problem algorithms in numerical simulations is a topic of current research.

CONCLUSION

The Schur algorithm, a fast algorithm that allows rapid data processing when discretized, has been applied to the inverse problem for a layered acoustic medium. Three different medium excitations were considered: impulsive plane waves at normal incidence; impulsive plane waves at oblique incidence; and an impulsive point source. For each excitation, the Schur algorithm was shown to decompose the pressure and vertical motion of the medium at each point into upgoing and downgoing waves, yielding the impedance of the medium as a function of travel time along a given ray path. For the latter two excitations, two Schur algorithms running in parallel with each other and with differential update equations were used to obtain separate profiles of the density and local speed of sound as functions of depth.

The use of the Schur algorithm seems to make the procedures of this paper computationally superior to that of the Gelfand-Levitan procedure used by Coen[4,5], for reasons explained at the end of Section II. In any case, the resolution of the medium motion into waves, and the dynamic deconvolution procedure associated with the Schur algorithm are interesting. More work needs to be done in testing these algorithms on actual data. In particular, their performance on noisy data is a subject of current research.

REFERENCES

1. J. Ware and K. Aki, "Continuous and Discrete Inverse-Scattering Problems in a Stratified Elastic Medium, Part I: Plane Waves at Normal Incidence," J. Acoust. Soc. Am. 45, 911-921 (1969).

2. R. Newton, "Inversion of Reflection Data for Layered Media: A Review of Exact Methods," Geophysics J. Royal Astr. Soc. 65, 191-215 (1981).

3. J. Berryman and R. Greene, "Discrete Inverse Methods for Elastic Waves in Layered Media," Geophysics 45(2), 213-233 (1980).

4. S. Coen, "Density and Compressibility Profiles of a Layered Acoustic Medium from Precritical Incidence Data," Geophysics 46(9), 1244-1246 (1981).

5. S. Coen, "Velocity and Density Profiles of a Layered Acoustic Medium from Common Source-Point Data," Geophysics 47(6), 898-905 (1982).

6. L. Faddeev, "Properties of the S-Matrix of the One-Dimensional Schrodinger Equation," Am. Math. Soc. Transl. Ser. 2 65, 139-166 (1967).

7. J. Claerbout, Fundamentals of Geophysical Data Processing, (McGraw-Hill, New York, 1976), p. 146.

8. E. Robinson, "Spectral Approach to Geophysical Inversion by Lorentz, Fourier, and Radon Transforms", Proc. IEEE 70(9), 1039-1054 (1982).

9. W. Symes, "Stable Solution of the Inverse Reflection Problem for a Smoothly Stratified Medium", SIAM J. Math. Anal. 12(3), 421-453 (1981).

10. F. Santosa and H. Schwetlick, "The Inversion of Acoustical Impedance Profile by Method of Characteristics", Wave Motion 4, 99-110 (1982).

11. K.P. Bube and R. Burridge, "The One-Dimensional Inverse Problem of Reflection Seismology", SIAM Review 25(4), 497-559 (1983).

12. A. Yagle and B. Levy, "The Schur Algorithm and its Applications," Tech. Report, Laboratory for Information and Decision Systems, Massachusetts Institute of Technology, Cambridge, MA. (November 1983).

13. P. Dewilde, J. Fokkema, and I. Widya, "Inverse Scattering and Linear Prediction, the Time Continuous Case," in Stochastic Systems: The Mathematics of Filtering and Identification and Applications, edited by M. Hazewinkel and J. Willems (D. Reidel, New York, 1981), pp. 351-382.

14. A. Bruckstein, B. Levy, and T. Kailath, "Differential Methods in Inverse Scattering," Tech. Report, Information Systems Laboratory, Stanford University, Stanford, CA. (June 1983), to appear in SIAM J. Applied Math.

15. K. Chadan and P. Sabatier, Inverse Problems in Quantum Scattering Theory (SPringer-Verlag, New York, 1977), p. 307.

16. M. Howard, "Inverse Scattering for a Layered Acoustic Medium using the First-Order Equations of Motion," Geophysics 48(2), 163-170 (1983).

17. A. Papoulis, Systems and Transforms with Applications in Optics, (McGraw-Hill, New York, 1968), p. 141.

18. A. Bultheel, "Towards an Error Analysis of Fast Toeplitz Factorization", Tech. Report No. TW-44, Applied Mathematics and Programming Division, Katholieke Universiteit Leuven, Belgium (May 1979).

FIGURE CAPTIONS

Fig. 1: The incident plane wave problem.

Fig. 2a: Recursion pattern for updating the downgoing waves.

Fig. 2b: Recursion pattern for updating the upgoing waves.

Fig. 3: The point source inverse problem.

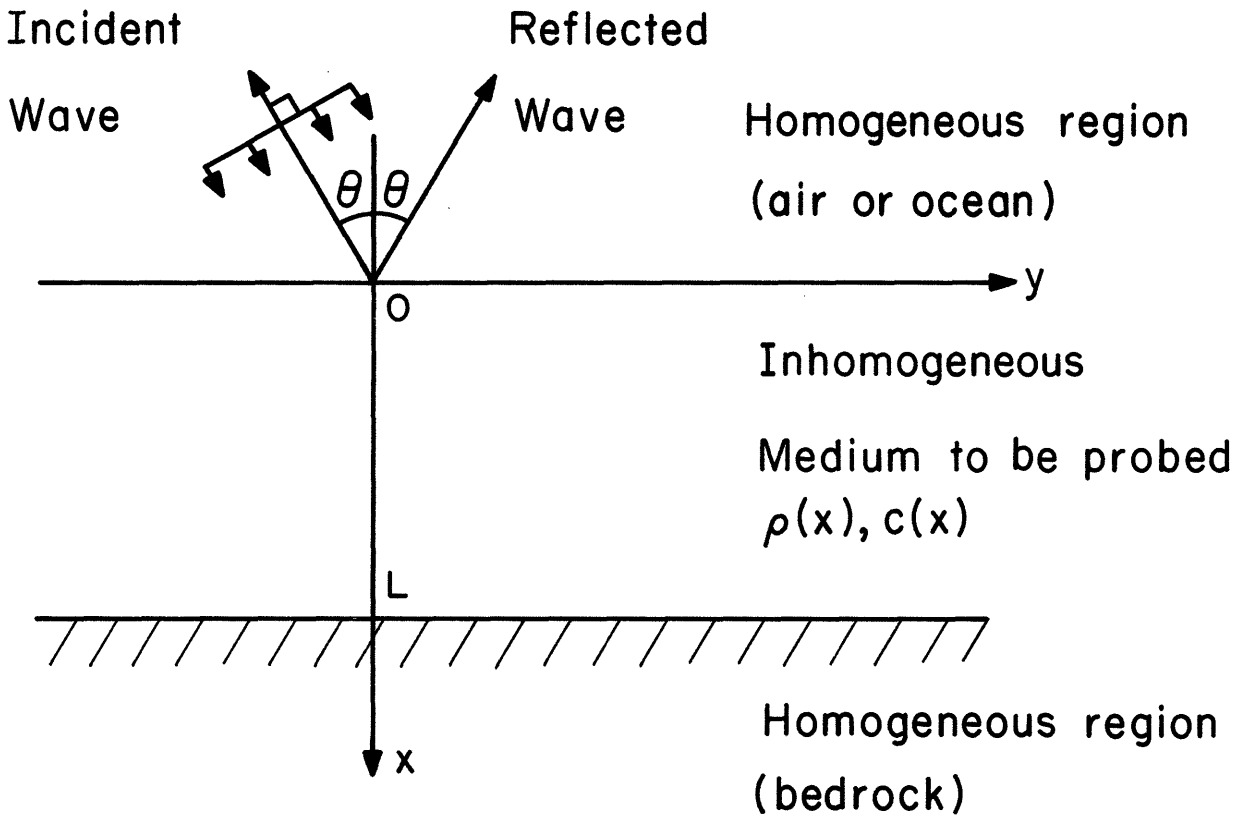

Fig. 1 The incident plane wave problem.

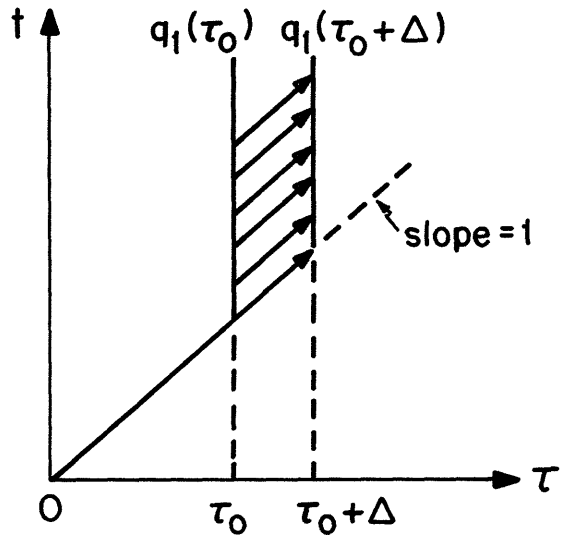

Fig. 2a: Recursions Pattern for Updating the Downgoing Waves

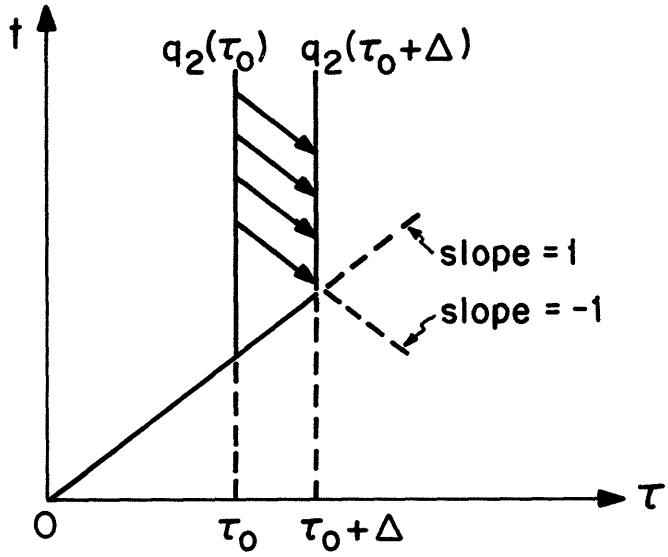

Fig. 2b: Recursion Pattern for Updating the Upgoing Waves

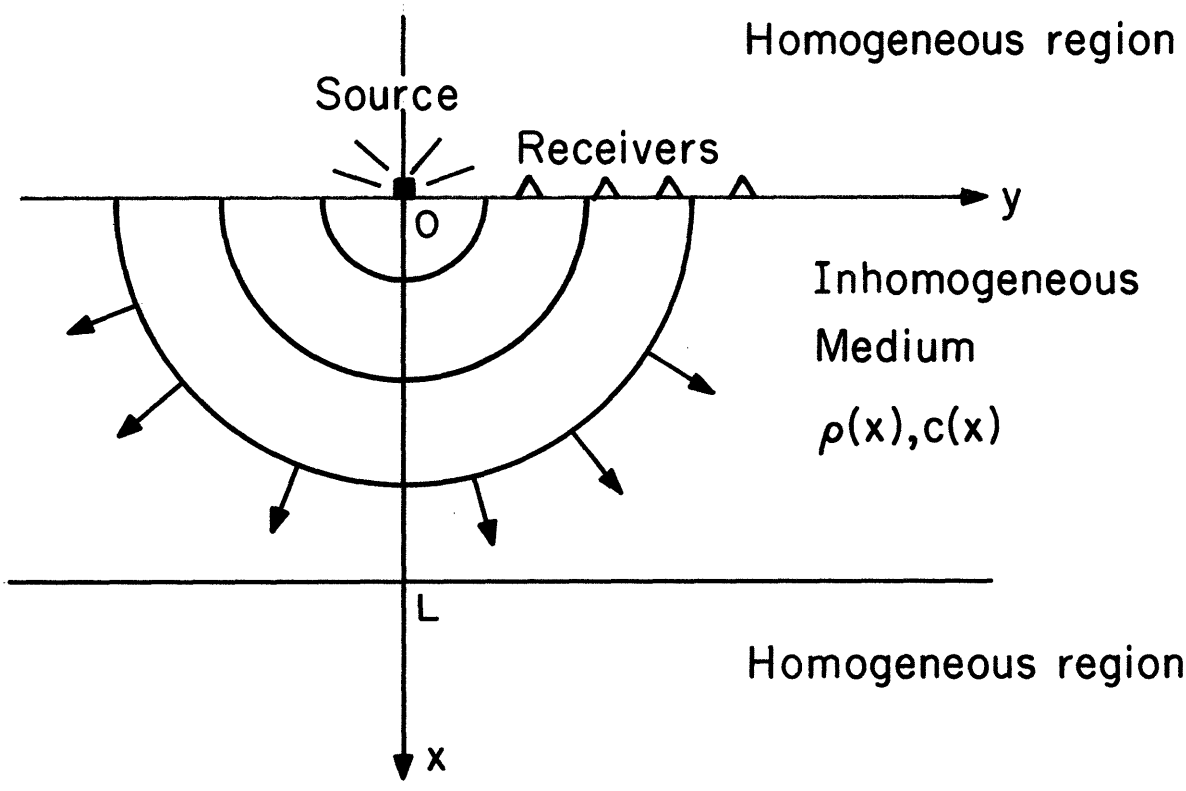

Fig. 3 The point source inverse problem